Published in final edited form as:

Neuron. 2016 May 4; 90(3): 609–621. doi:10.1016/j.neuron.2016.03.033.

Oxytocin Enhances Social Recognition by Modulating Cortical Control of Early Olfactory Processing

Lars-Lennart Oettl[1], **Namasivayam Ravi**[1], **Miriam Schneider**[1], **Max F. Scheller**[1], **Peggy Schneider**[1], **Mariela Mitre**[2], **Miriam da Silva Gouveia**[3], **Robert C. Froemke**[2], **Moses V. Chao**[2], **W. Scott Young**[4], **Andreas Meyer-Lindenberg**[1], **Valery Grinevich**[1,3], **Roman Shusterman**[5,6], and **Wolfgang Kelsch**[1,*]

[1]Central Institute of Mental Health, Medical Faculty Mannheim, Heidelberg University, 68159 Mannheim, Germany

[2]Skirball Institute for Biomolecular Medicine, New York University School of Medicine, New York, NY 10016, USA

[3]German Cancer Research Center, 69120 Heidelberg, Germany

[4]Section on Neural Gene Expression, National Institute of Mental Health, NIH, Bethesda, MD 20892, USA

[5]Sagol Department of Neurobiology, University of Haifa, Haifa 3498838, Israel

SUMMARY

Oxytocin promotes social interactions and recognition of conspecifics that rely on olfaction in most species. The circuit mechanisms through which oxytocin modifies olfactory processing are incompletely understood. Here, we observed that optogenetically induced oxytocin release enhanced olfactory exploration and same-sex recognition of adult rats. Consistent with oxytocin's function in the anterior olfactory cortex, particularly in social cue processing, region-selective receptor deletion impaired social recognition but left odor discrimination and recognition intact outside a social context. Oxytocin transiently increased the drive of the anterior olfactory cortex projecting to olfactory bulb interneurons. Cortical top-down recruitment of interneurons dynamically enhanced the inhibitory input to olfactory bulb projection neurons and increased the signal-to-noise of their output. In summary, oxytocin generates states for optimized information extraction in an early cortical top-down network that is required for social interactions with potential implications for sensory processing deficits in autism spectrum disorders.

*Correspondence:wolfgang.kelsch@zi-mannheim.de.

[6]Present address: Institute of Neuroscience, University of Oregon, Eugene, OR 97403, USA

SUPPLEMENTAL INFORMATION

Supplemental Information includes Supplemental Experimental Procedures and eight figures and can be found with this article online at http://dx.doi.org/10.1016/j.neuron.2016.03.033.

AUTHOR CONTRIBUTIONS

Conceptualization, W.K., L.-LO., N.R., M.F.S., M.S., and R.S.; Methodology, W.K., L.-LO., M.F.S., M.S., and R.S.; Investigation, W.K., M.S.G., L.-L.O., N.R., M.F.S., M.S., and P.S.; Writing - Original Draft, W.K., L.-L.O., and A.M.-L.; Writing - Review & Editing, V.G., W.K., L.-L.O., and W.S.Y.; Funding Acquisition, W.K.; Resources, R.C.F., M.V.C., V.G., W.K., M.M., A.M.-L., and W.S.Y.; Supervision, V.G., W.K., M.S., and R.S.

INTRODUCTION

Efficient extraction of sensory information from conspecifics is critical to social recognition across perceptual boundaries throughout evolution, from olfaction in rodents and other animals to vision in humans (Brennan and Kendrick, 2006). Social recognition has been classically studied in rodents and other mammals (Fleming et al., 1979; Sanchez-Andrade and Kendrick, 2009; Wiesner and Sheard, 1933). Information on the identity of the conspecific comes from olfactory cues in urine or secretions from skin, reproductive tract, or specialized scent glands (Mykytowycz and Goodrich, 1974; Natynczuk and Macdonald, 1994; Stopka et al., 2007). The recognition of social olfactory cues is dependent on an intact main olfactory system since lesions of the main olfactory bulb (MOB) or chemically induced anosmia impair individual recognition in rodents (Dantzer et al., 1990; Popik et al., 1991; Sanchez-Andrade and Kendrick, 2009).

Odor information from the olfactory sensory neurons is first processed in MOB projection neurons, i.e., mitral and tufted cells (M/TCs), which convey sensory inputs directly to the olfactory cortex. Odor coding in M/TCs is modulated by inter-neuron networks. The most abundant interneurons are granule cells (GCs). GCs receive massive cortical top-down inputs primarily from the anterior olfactory nucleus (AON), which is the most anterior portion of the olfactory cortex (Balu et al., 2007; Brunjes et al., 2005; Cajal, 1911; de Olmos et al., 1978; Haberly and Price, 1978; Kerr and Hagbarth, 1955; Luskin and Price, 1983; Shipley and Adamek, 1984). These top-down inputs are transiently active in a brain-state-dependent manner (Boyd et al., 2015; Otazu et al., 2015; Rothermel and Wachowiak, 2014) and increase GC firing, thereby modulating inhibition on M/TCs (Balu et al., 2007; Boyd et al., 2012; Markopoulos et al., 2012). It is not known whether and how top-down inputs control odor coding relevant to social interactions.

The oxytocin (OXT) system is a critical modulator to social perception and behaviors (Lee et al., 2009). OXT release to the forebrain originates from neurons in the paraventricular nucleus (PVN) of the hypothalamus. The mechanisms have not been resolved through which OXT acts on olfactory circuits (Insel, 2010; Kendrick et al., 1992; Numan and Insel, 2003; Yu et al., 1996). The rat MOB itself contains few OXT terminals and OXT receptors (OXTRs), with the least dense expression in the GC layer (Numan and Insel, 2003; Vaccari et al., 1998). Interestingly, the AON is among the brain regions with highest OXTR expression (Freund-Mercier et al., 1987; Tribollet et al., 1988; Vaccari et al., 1998; Yoshimura et al., 1993) and receives dense innervation from OXT neurons of the PVN (Knobloch et al., 2012).

The main olfactory system is used both for social and nonsocial information processing (Numan and Insel, 2003; Sanchez-Andrade and Kendrick, 2009). We tested the hypothesis that OXT may set the main olfactory system into a specific state for processing of social odor cues. Context-dependent modulation of early olfactory activity is observed through different top-down mechanisms (Doucette et al., 2011; Kay and Laurent, 1999; Linster and Fontanini, 2014). We speculated that OXT may generate context-dependent signal processing states in the MOB through transient activation of AON top-down projections to promote extraction of relevant information. Indeed, we found that OXT activated the AON

and its top-down projections to GCs in the MOB to dynamically enhance the signal-to-noise ratio of odor responses in vivo. At a behavioral level, optogenetically evoked OXT release enhanced olfactory exploration of conspecifics and improved later social recognition, while the deletion of OXTRs in the AON impaired recognition.

RESULTS

Endogenous OXT Release Promotes Olfactory Exploration and Future Conspecific Recognition

First, we tested the hypothesis that evoked endogenous OXT release modifies olfactory exploration behavior during same-sex conspecific interaction and impacts future recognition of the conspecific. Toward this aim, we performed an olfaction-and OXT-dependent social recognition task in female adult Wistar rats (Engelmann et al., 1998; Popik et al., 1991).To evoke OXT release, a light-activatable opsin, Channelrhodopsin2 (ChR2), was expressed selectively under the control of an OXT promoter fragment in OXT neurons of the PVN following bilateral virus injection ($rAAV_{1/2}$-OXT-ChR2:mCherry) (Knobloch et al., 2012) (Figure 1A). In rats, ChR2:mCherry expression was confined to PVN neurons immunoreactive to OXT (Figures 1B, S1A, and S1B, available online) with 98%–100% cell-type specificity, as reported in Knobloch et al. (2012). Littermate rats served as controls and expressed only a green fluorescent protein ($rAAV_{1/2}$-OXT-vGFP). The task consisted of a 5 min long initial sample phase with a same-sex juvenile conspecific (Figure 1C). During the sample phase, 30 Hz blue laser pulses (duration 20 s) were repeated every minute and applied to PVN through optic fibers both in adult $ChR2^+$ and control rats (Figure S1C). Anogenital exploration is considered critical for olfactory sampling of con-specifics (Miczek and de Boer, 2005). During the sample phase, single anogenital investigation events and their total duration were longer in $ChR2^+$ animals than in control rats (Figures 1D– 1F), while the two groups did not differ in the frequency of anogenital explorations or other forms of interaction (Figures 1D and S1D). These observations suggested that OXT enhanced the intensity of olfactory exploration behaviors during social investigation.

Rats do not recognize the former interaction partner if the interval between sample and re-exposure phase exceeds 1 hr (Dantzer et al., 1987). To test for enhancement of conspecific recognition through OXT, we increased the interval to the recognition phase to 2 hr. During the subsequent social recognition phase, adult rats were exposed to the previous juvenile interaction partner and a new juvenile for another 3 min without laser stimulation. During the social recognition period, rodents prefer the novel over the familiar partner and express increased exploratory behavior toward the unknown conspecific. After the 2 hr interval, control rats explored their interaction partners at chance level (Figure 1G). In contrast, $ChR2^+$ rats explored the novel conspecific more than the previous interaction partner. The total exploration time did not differ between $ChR2^+$ and control rats (Figure S1D). Also, evoked OXT release had no effect on object recognition (Figure S1E). Thus, evoked OXT release promotes a state of increased olfactory exploration and improved recognition. We therefore wondered how OXT may modify early olfactory coding states relevant to information processing.

OXT Activates GC Inhibition through Activation of Top-Down Projections from AON

OXTRs are highly expressed in the AON (Tribollet et al., 1988; Vaccari et al., 1998). The AON provides dense glutamatergic top-down projections to the MOB and could thereby control early olfactory processing. Initially, we made whole-cell recordings in acute brain slices to determine the relative fraction of neuron types based on their firing pattern in the adult rat AON (Figures 2A and S2A–S2G). We observed that the majority of neurons had pyramidal-shaped cell bodies and a regular, adapting firing response (Figures S2A and S2B). A smaller fraction of cells showed a burst- or fast-firing pattern (Figures S2C and S2D). In a total of 85 AON neurons, we determined how OXT affects the spontaneous rate of inhibitory and excitatory postsynaptic currents (sEPSCs and sIPSCs). The [Cl] in the pipet was set so that glutamatergic CNQX-sensitive sEPSCs were detected as inward currents and $GABA_A$R-mediated gabazine-sensitive sIPSCs as outward currents at V_h = −60 mV (Figure S2H). We then applied brief pulses of the selective OXTR peptide agonist [Thr4,Gly7]-oxytocin (TGOT; 1 μM) (Elands et al., 1988) locally onto AON neurons (Figure 2B). TGOT reversibly increased the sEPSC frequency in regular-firing AON neurons (Figures 2C–2F). In line with OXTR activation driving the AON, sIPSC rates also increased in AON cells (pre, 0.84 ± 0.61 Hz; TGOT, 4.21 ± 1.06 Hz; post, 0.88 ± 0.47; n = 7, ANOVA, p = 0.003), and increases in the sEPSC rate were also observed in AON fast-spiking neurons (Figure 2G). These increases in glutamatergic synaptic activity were still observed when $GABA_A$Rs were blocked by gabazine (10 μM) (Figure 2H), indicating that the inhibition was not required for OXT to drive the AON network. The increases in synaptic drive could be repeatedly evoked by TGOT (Figures 2E and S3A) and independent of the rats' sex (Figures S3B and S3C).

We then tested whether optogenetically induced endogenous OXT release from axon terminals of $ChR2^+$ PVN neurons would equally drive the AON network (Figure 3). Indeed, the same stimulation protocol used for behavioral experiments (5 ms pulses at 30 Hz for 2–20 s; Figure 3A) evoked transient sEPSC rate increases in regular-firing cells (Figures 3B, 3C, and S3D) that in some cells were paralleled closely by increases in sIPSC rates (Figures 3D and 3E). Both increases in sEPSC and sIPSC drive were reversibly blocked by the selective OXTR peptide antagonist OTA (1 μM; Figure 3C). At least 2-fold increases in the synaptic drive both through OXTR agonist and evoked endogenous OXT release were observed in the majority of the recorded cells (Figure S3F) independent of their baseline sEPSC input rates (29 nonresponders, 0.37 ± 0.07 Hz versus 56 responders, 0.42 ± 0.05 Hz; t test, p = 0.29). To examine the extent of OXTR expression in AON neurons projecting to the MOB, we used a virus that infects neurons retrogradely (CAV2-Cre) (Beier et al., 2015). CAV2-Cre virus was injected into the GC layer of the MOB of mice that express dTomato only upon Cre recombination (Ai9:dTomato mice; Figures 3F and S3G). In support of broad recruitment of the AON circuit, 1,069 of 1,078 $dTomato^+$ AON neurons were immunoreactive for the OXTR.

We finally tested whether OXTR activation modified the firing threshold of regular-firing AON neurons (Figure 4). TGOT reversibly decreased the firing threshold of regular-firing AON neurons independent of fast synaptic transmission (CNQX [10 μM], D-AP5 [50 μM], and gabazine [10 μM]; Figures 4A–4C and S4) and without significantly changing the

neuronal resting membrane potential (Figure S4A), presumably by regulating the activity of ionic membrane channels as described in other brain regions (Raggenbass, 2001). In line with this observation, application of the fast sodium channel blocker TTX (1 μM) blocked TGOT-evoked EPSC rate increases in the AON (Figures 4D and 4E). Thus, these data support that OXT released to the AON increased excitability of regular-firing neurons and the global excitatory synaptic drive.

Assuming that increased AON excitation will propagate to the MOB through top-down projections, we tested whether local TGOT application to the AON would increase synaptic input to the MOB. In the MOB, AON projections preferentially target the perisomatic region of GCs. Indeed, the rate of sEPSC inputs increased in GCs when TGOT was applied to the AON, while inhibitory events did not change (Figures 5A–5C and S5A). GCs receive two types of EPSC inputs: perisomatic EPSC inputs with fast kinetics and EPSC with slow kinetics that preferentially arrive in the distal domain where GCs form contacts with M/TCs in the external plexiform layer (Balu et al., 2007; Kelsch et al., 2008; Nissant et al., 2009; Schoppa, 2006). Indeed, direct optogenetic excitation of $ChR2^{+}$ AON neurons elicited fast evoked (e) EPSCs in GCs (Figures 5D and 5E). In line with AON projections preferentially targeting GCs in the MOB, TGOT application resulted in a selective increase in sEPSCs with fast decay kinetics (Figures 5F–5H). The increase in fast sEPSCs onto GCs was blocked when the connection between the AON and MOB was lesioned and TGOT directly applied to the MOB (Figures 5I– 5K), compatible with OXT acting in the rat AON, but not the MOB. Finally, we recorded from mitral cells that are the main output of GCs (Figures 5L–5N). As expected, TGOT in the AON reversibly increased the sIPSC rate in mitral cells. However, cortical OXTR activation did not elicit a brief excitation of mitral cells with fast desensitization (Figure S5B) as can be observed with direct, global excitation of AON neurons (Boyd et al., 2012; Markopoulos et al., 2012). In summary, OXT activates excitatory top-down projections from the AON to GCs that in turn increased inhibitory input to mitral cells (Figure 5O).

Modulation of Odor Coding through Top-Down OXT Action

We then tested how OXT modifies odor coding in M/TCs of the olfactory bulb through AON top-down control (Figure 6A). We performed in vivo recordings in anesthetized rats that allowed for local infusion of the OXTR agonist into the AON to study the consequences of local OXT actions rather than brain-wide optogenetic effects. OXT can modify the sniffing frequency (Wesson, 2013). The sniffing frequency affects odor response in M/TCs (Carey and Wachowiak, 2011). We took advantage of the fact that the sniff rate is clamped in anesthetized rats to isolate top-down effects of OXT on M/TCs through AON top-down projections (Figures 6B, 6C, S6A, and S6B). Multiple odorants were presented in a randomly alternating fashion in the same session. M/TCs were recorded while monitoring the respiration cycle. Alignment of the odorant-evoked M/TC firing response to the sniff or breathing cycle yielded a defined on- and offset of the firing response to 0.5 s of odorant application (Figures S6C–S6F). We analyzed M/TCs that displayed increases in the firing rate to at least one odorant before application of the OXTR agonist TGOT (Figure 6D). M/TC units responded on average to two-thirds of the three odorants that had been applied randomly throughout the recording (Figures 7A–7G). For the 20 detected cell-odor pairs,

OXTR activation through TGOT in the AON reversibly increased the signal-to-noise ratio of the odor responses (Figure 7C), defined as the stimulus-evoked activity relative to the spontaneous activity (Hurley et al., 2004). During the OXT effect, the baseline firing rate of M/TCs decreased (Figure 7D) and the peak firing response to odorants increased (Figure 7E). Also, at 10-fold lower odorant concentrations, TGOT robustly increased the peak odor response (Figures S7A and S7B). TGOT did not significantly change the time of onset of the odor response relative to the sniff cycle or the duration of the odor response (Figure S7C).

To visualize the changes in signal-to-noise ratio for each cell-odor pair, we calculated the modulation index (MODI), defined as (firing $rate_{response}$ − firing $rate_{baseline}$)/(firing $rate_{response}$ + firing $rate_{baseline}$) (Otazu et al., 2009). TGOT increased the MODI broadly throughout the applied odorants (Figures 7F and 7G). Cells that did not respond to an odor before TGOT also did not increase their firing rate during odorant application through OXTR agonist application to the AON (Δ(TGOT − Pre) = −10.9 ± 8.5 Hz; p = 0.5, t test, n = 10).

To determine the relationship between the signal-to-noise ratio of M/TCs and OXTR recruitment in the AON, we varied the amount of applied OXTR agonist. In total, 3-fold lower TGOT concentrations still increased the signal-to-noise ratio (Figures 7H-7K). Yet the effects became globally weaker. Even though the “low” TGOT did not anymore significantly decrease the baseline firing activity (Figure 7L), it still had some effect on the peak odor response when all cell-odor pairs were pooled (Figure 7M). Since $MODI_{TGOT}$ did not increase across all cell-odor pairs (Figure 7N), we speculated that the effect of low TGOT is not expressed in all cell-odor pairs to an equal extent. Initially weak responses (low $MODI_{pre}$) are expected to have a larger dynamic range to boost $MODI_{TGOT}$. Indeed, $MODI_{TGOT}$ increased for odors with lowest respective $MODI_{pre}$ in each cell, but not for odors with the next higher $MODI_{pre}$ (Figure 7O). We then tested whether $MODI_{pre}$ also predicts peak odor response behavior following low TGOT. Indeed, the normalized peak odor response only increased significantly for odors with the lowest $MODI_{pre}$ (Δ = +30.7% ± 12.8%; $p < 0.05$), but not for corresponding odors with the next higher $MODI_{pre}$ (Δ = +14.8% ± 15.4%; n.s., t test) in the seven cells that responded to two odors.

While recording in the deep layers of the MOB, we also found units that had properties of interneurons, presumably GCs with low baseline firing that was not modulated by the respiration cycle (Cang and Isaacson, 2003). In these eight units, TGOT application to the AON transiently increased the firing rate (Figure S7D) as predicted for increased excitatory drive through top-down inputs. In summary, we observed that OXTR activation in the AON induced a transient state of increased signal-to-noise of evoked odor responses in MOB projection neurons through mechanisms that are compatible with increased GC inhibition through top-down inputs.

Requirement of OXTR Activation in the AON for Social Recognition

We finally tested whether specific deletion of OXTRs in the AON affects social recognition. These experiments were performed in mice as they allow for conditional gene deletion selective to the AON ($OXTR^{\Delta AON}$). To generate $OXTR^{\Delta AON}$ mice, $rAAV_{1/2}$-CBA-Cre was injected in the AON of mice in which the OXTR gene was flanked by loxP sites (Figures 8A

and S8A). Control mice received the same virus injection but had two wild-type OXTR alleles. The mice underwent the same-sex social recognition task. This task is established in single-housed male mice (Kogan et al., 2000) that can remember the other animal for an interval of 30 min between the sample and recognition phase. Consistent with the requirement of OXTRs in the AON for olfaction-dependent social interaction, we observed a deficit in recognition of conspecifics in $OXTR^{\Delta AON}$ mice in comparison to control mice (Figures 8B and 8C). Importantly, $OXTR^{\Delta AON}$ mice spent more time investigating conspecifics during the initial sample phase than control mice (Figure 8B) and displayed a similar trend in the recognition phase (Figure S8B), indicating that the memory deficit did not derive from reduced social interaction. However, $OXTR^{\Delta AON}$ mice performed object and nonsocial odor recognition similarly to control mice (Figures 8D and S8C–S8E). Also, $OXTR^{\Delta AON}$ and control mice had comparable abilities to discriminate progressively more similar binary odor mixtures (Figures 8E and 8F), together supporting that OXTRs in the AON become relevant in situations when social cues have to be processed.

DISCUSSION

This study describes a novel circuit mechanism for OXT release to the olfactory cortex that modifies the state of early odor coding through dynamic top-down control. These top-down inputs increased the inhibitory tone to MOB projection neurons, thereby improving the signal-to-noise of odor responses. These findings demonstrate that OXT modifies olfactory coding already at early stations of bottom-up sensory information processing, and that OXT actions in an early sensory cortical top-down system are required for social recognition.

Top-Down Control in Olfaction

Pioneering descriptions (Davis et al., 1978; Wallenberg, 1928) speculated that top-down projections from AON to MOB “may permit more central structures to coordinate olfactory processing with ongoing behavior and endocrine or nutritional requirements” (Davis et al., 1978). For instance, food odors evoked higher M/TC firing responses in hungry rats than satiated animals (Pager et al., 1972). Top-down projections have been implicated in state-dependent modulation of olfactory bulb activity (Kerr and Hagbarth, 1955; Pager et al., 1972; Soria-Gómez et al., 2014; Wallenberg, 1928; Yamaguchi et al., 2013). These and other studies had, however, not addressed how AON top-down inputs modify odor processing in this or other behaviors, including social interaction. We now observed that endogenous OXT release and OXTR agonists increased transiently the intrinsic excitability of AON regular-firing neurons and the excitatory synaptic drive in the AON network. GCs are the main target of AON axon terminals in the MOB, with deep parts of the GC layer receiving a higher density of top-down fibers (Laaris et al., 2007; Luskin and Price, 1983). Indeed, AON excitation through OXT propagated through top-down projections to increase glutamatergic synaptic input to GCs. In vivo, we also found putative GC units that displayed transient increases in their firing rate following OXTR activation in the AON. Along with GCs innervating primarily M/TCs, OXT in the AON increased the inhibitory drive to M/TCs. Together, these findings reveal a novel pathway for OXT that increases the excitability of AON top-down projections that drive olfactory bulb interneurons for inhibition of M/TCs.

States of Enhanced Signal-to-Noise in Odor Coding

Efficient sensory neural codes in single neurons are predicted to be sparse (Barlow, 1961; Olshausen and Field, 2004; Willmore and Tolhurst, 2001). Compatible with OXT promoting information extraction, OXTR activation in the AON in vivo enhanced the signal-to-noise ratio by lowering baseline firing of M/TCs and by increasing their peak odor responses. Actions of OXT on neural coding were recently also observed in hippocampal in vitro recordings (Owen et al., 2013). In their study, OXT enhanced hippocampal spike transmission by modulating interneurons and improved the signal-to-noise ratio. It is therefore possible that modification of information transfer through induction of high signal-to-noise states is a shared feature of OXT in different systems. OXT release in the auditory cortex, amygdala, and hippocampus also works primarily through modulation of interneuron activity (Huber et al., 2005; Marlin et al., 2015; Owen et al., 2013).

In the MOB, several mechanisms can modify the signal-to-noise in odor coding through increased interneuron activity that is driven by cortical top-down inputs. OXTR recruitment in the AON increased the signal-to-noise of odor responses through increasing peak firing responses to odors and reduced background firing activity. During this state of increased signal-to-noise, GCs also increased firing, compatible with glutamatergic AON projections mainly targeting GCs in the MOB.

Glutamatergic top-down inputs from the cortex can impact activity of M/TCs in different ways. Broad optogenetic excitation of AON neurons suppresses both baseline firing and odor responses (Markopoulos et al., 2012), while stimulation of anterior piriform cortex top-down projections only suppresses odor responses, but not baseline firing, in M/TCs (Boyd et al., 2012). Both studies found that beyond GCs, interneurons in the glomerular layer were also activated. In contrast to these two studies, direct optogenetic excitation of GCs lowers baseline firing while strengthening odor responses in M/TCs (Alonso et al., 2012). Importantly, and different from broad optogenetic activation of olfactory cortices, OXT in the AON, which efficiently recruits GCs in the MOB, had similar effects as direct GC excitation. Compatible with different subcircuits existing in the early olfactory cortices, all subregions of the AON project primarily to the GC layer of the MOB(Brunjes et al., 2005). Only some subregions also project to the external plexiform of the glomerular layer (Brunjes et al., 2005). Periglomerular neurons mostly suppress odor responses, while external tufted cells are also suited to amplify odor responses of M/TCs (Boyd et al., 2012; Brunjes et al., 2005; De Saint Jan et al., 2009; Hayar et al., 2004; Markopoulos et al., 2012). Together, these observations suggest that the actions of top-down projections can have different functions on M/TC firing depending on which subcircuits are activated in the early olfactory cortices as exemplified by the different actions of broad AON activation through direct optogenetic stimulation and modulation of AON activity through a physiologic agonist.

The GC-M/TC network has features that allow for increasing firing of stimulus-driven inputs while suppressing weak activity as occurs during baseline firing, depending on the strength of inhibition from GCs. M/TCs are neurons with burst-firing properties. Increases in inhibitory input within a certain range bring voltage-dependent conductances in a different state so that the regenerative conductances result in more intense burst discharges in response to a given stimulus (Angelo et al., 2012; Balu and Strowbridge, 2007). When the

effect became globally weaker, moderate OXTR recruitment in the AON still increased the signal-to-noise of odor responses. In this condition, the effect of inhibitory input on baseline firing of M/TCs became negligible. Biophysical properties of M/TCs derived from in vitro studies suggest that subtle increases of GC inhibition can boost stimulus-driven odor responses of M/TCs (Angelo et al., 2012; Balu and Strowbridge, 2007). Compatible with these M/TC properties, moderate OXTR recruitment in the AON still increased peak firing responses to odors. Compatible with the larger dynamic range of initially small odor responses, moderate recruitment of top-down projections through OXT preferentially amplified those weaker odor responses. Stronger GC recruitment continues to increase burst odor responses and then also significantly reduces baseline firing of M/TCs (Alonso et al., 2012). Indeed, stronger OXTR activation in the AON reduced background firing and amplified peak odor responses of M/TCs. Finally, in line with increases in GC inhibition only boosting stimulus-driven burst responses, M/TCs that did not respond to an odor before OXTR activation in the AON also did not respond to that odor following recruitment of top-down projections.

The OXT-induced state is predicted to promote stimulus selection and information extraction and thereby facilitates memory formation. Barlow (1961) predicted two aspects that relate to the here observed OXT actions, i.e., sparsening in M/TC coding of sensory information and the existence of sensory relays that modulate the flow of information according to requirements of other parts of the brain. This second concept matches the top-down control of early sensory information flow with respect to the current state of the animal during brain-wide modulation through OXT. The main olfactory system is used both for social and nonsocial information processing. The prosocial peptide is released preferentially during interactions with conspecifics (Lukas and Neumann, 2013). OXT effects on olfactory processing are therefore predicted to primarily affect social cues under natural conditions. Indeed, OXTR deletion in the AON selectively affected olfaction-dependent sampling behavior and recognition of conspecifics, but not odor discrimination or recognition outside a social context. Together, these observations argue for a modulatory system that is specialized to come into action for sensory processing of social information.

Sensory Processing in Social Interaction and Recognition

Our findings support that one of the major functions of central OXT is to bring multiple levels of sensory-, motor-, and emotion-regulating systems into a state for social interaction. Exploration of conspecifics is promoted through more intense olfactory sampling of conspecifics found in this study and a low anxiety state induced by nonsensory systems (Lukas et al., 2011; Viviani et al., 2011). At the level of sensory processing, OXT modifies the state of early olfactory presentation that may enhance salience of concurrently presented odors and help to detect relevant information of conspecifics during social encounters. Compatible with this idea, a possible reason for the longer conspecific exploration times in mice with OXTR deleted in the AON could be less efficient information extraction due to OXT's effects on the gain of odor representations. Through its cortical top-down projections into the early olfactory system, OXT modifies the global gain control of olfactory coding before MOB output spreads into divergent higher-order pathways including the posterior piriform cortices, the ventral striatum (olfactory tubercle), the amygdala, and the entorhinal

cortices (Igarashi et al., 2012; Sosulski et al., 2011). Many of these higher-order brain regions are activated during social interactions and also express OXTRs (Dölen et al., 2013; Kim et al., 2015; Vaccari et al., 1998), allowing for further modifications of information through OXT during particular types of social behavior. It is likely that storage of recognition memory involves distributed circuits. For instance, in the posterior piriform cortex, OXT promotes formation of association learning of an initially neutral odor with a potential mating partner (Choe et al., 2015). Other-and same-sex investigation and recognition may be regulated through different mechanisms. For instance, OXT-deficient male mice display normal initial other-sex exploration but impaired recognition that could be rescued by OXT infusion into the amygdala (Ferguson et al., 2001). Interestingly, OXT treatment was only effective preceding the initial investigation. While local OXTR activation in the amygdala is critical to other-sex recognition, it was found to be less so to same-sex recognition (Lukas et al., 2013). Along with OXT simultaneously modifying multiple levels of the olfactory system, future studies may address if OXT also modulates association fibers from the AON to other cortical areas in addition to the here described top-down projections. The present study focused on the transient OXT-activated top-down modification of early sensory processing. Region-specific deletion of OXTRs supports the requirement of the AON in OXT-mediated modulation of sensory information relevant to olfactory investigation of conspecifics and their future recognition.

Finally, more research is needed to address the potential clinical implications of our data. From olfaction in rodents to vision in humans, the role of OXT in social recognition is conserved across evolution within the dominant sensory modalities of species (Lee et al., 2009). Like humans, monkeys use vision and auditory cues as primary modalities for social communication. In monkeys, OXTR is enriched in the subcortical and early cortical visual areas and cholinergic nuclei controlling sensory processing in these modalities, suggesting the involvement of OXT in a variety of functions relevant to social cognition, including modulating visual attention, processing, and sensory stimuli (Freeman et al., 2014a, 2014b). In humans, the OXT system is thought to be affected in social disorders such as autism, and it has been shown that OXT can ameliorate some of the related deficits in social interaction (Meyer-Lindenberg and Tost, 2012). Notably, aberrant sensory processing is a core aspect of autism spectrum disorders (American Psychiatric Association, 2013; Asperger, 1944; Crane et al., 2009; Domes et al., 2013; Markram and Markram, 2010; Skuse et al., 2014) and includes atypical neural responses at early stages of perceptual processing (Robertson et al., 2014). Since species-specific variations of the identified OXT-dependent control mechanism may be effective in humans, this line of research may provide a plausible mechanism and entry point for both the pathophysiology and treatment of early social sensory processing deficits in humans.

EXPERIMENTAL PROCEDURES

Animals and Husbandry

Wistar rats were obtained from Harlan-Winkelmann and group housed at a 12 hr day-and-night-cycle. $OXTR_{fl/fl}$ mice (RRID: IMSR_JAX:008471) (Lee et al., 2008) and Ai9:dTomato reporter (RRID: IMSR_JAX:007905) (Madisen et al., 2010) were maintained

in a C57BL/6J (Charles-River) background. All procedures were approved by the local animal welfare committee and in accordance with NIH guidelines.

Behavioral Analyses

Social Recognition in Rats—The social recognition task was performed in group-housed female adult 13-week-old Wistar rats, 4 weeks after they had been injected with $rAAV_{1/2}$-OXT-ChR2:mCherry in the PVN. Control animals were injected with $rAAV_{1/2}$-OXT-vGFP. Both groups were implanted with optic fibers into the PVN directly following virus injection. Social interaction partners were of the same sex and 4–5 weeks old. Adult rats were placed in an open field (50 cm × 50 cm × 45 cm) and exposed to an unknown social partner (A) for 5 min during the initial sample phase. During the sample phase, the adult rat received 5 ms long blue laser pulses for 20 s at 30 Hz every minute. After this 5 min session, the adult animal returned to its home cage for 2 hr. This interval was chosen so that control rats performed at chance level. In the recognition test phase, the adult rat was placed again in the open field for 3 min without laser stimulation. The familiar (A′) and a novel social partner (B) were presented to the experimental animal.

The social investigation times and frequency, as well as the frequency of anogenital, nonanogenital, and following events during the initial sample phase, were quantified offline by a trained experimenter blinded to group assignment. Other social behaviors, such as grooming, crawl over, or social play, were not scored as social investigation. Social recognition was quantified as the percentage of social recognition memory, i.e., [time of investigation of new partner B/(time of investigation of new partner B + time of investigation of familiar partner A′)] expressed in percent. No significant interaction was found for social recognition or investigation for the stage of estrous cycle that was determined through vaginal smear (data not shown), in line with previous observations that olfactory perception and motivation is not affected by the estrous cycle (Sánchez-Andrade et al., 2005).

Social Recognition in $OXTR^{\Delta AON}$ Mice—The social recognition task was performed in single-housed adult 12-week-old male $OXTR^{\Delta AON}$ mice or control littermate mice. Animals were examined 5 weeks after $rAAV_{1/2}$-CBA-Cre injection into the AON. The social recognition task was performed and analyzed as described for rats. The interval between sample and recognition phase was shortened as memories are retained for 30 min in single-housed mice (Kogan et al., 2000).

Slice Electrophysiology

Whole-cell recordings were performed in acute slice preparation from at least 8-week-old rats.

In Vivo Electrophysiology

At least 8-week-old rats were anesthetized with urethane (1.5 g/kg intraperitoneally [i.p.]) and placed in a stereotactic apparatus. Body temperature was maintained with a heat pad (WPI). Craniotomy was performed over the MOB and AON. M/TC activity in the MOB was recorded with glass-coated tungsten microelectrodes (0.5 MΩ, Alpha-Omega). Cells were preferentially recorded from the ventral mitral cell layers for reasons of better long-term

stability. The same results were, however, obtained also from M/TC units in the dorsal MOB. For identification of M/TCs, the criteria used were recording depth, firing activity that synchronized to respiration frequency, and odor-evoked responses (Rinberg et al., 2006). A glass micropipette filled with the selective OXTR agonist TGOT (1 μL, 0.5 or 1.6 μM), dissolved in ACSF, and connected to a nano-injector (MO-10, Narishige) was simultaneously inserted into the AON. The agonist was then applied after establishing a baseline of odor-evoked responses. Coordinates for stimulation were as follows (in mm relative to Bregma): anterior 5.1, lateral 2.2, ventral 5.2, and lateral angle of 10°. Breathing signals were either monitored with a pressure sensor (24PCEFJ6G, Honeywell) via a stainless steel cannula implanted through the bone into the nasal cavity, or by placing a reflectance sensor carrying an infrared LED and phototransistor pair (QTR-1A, Pololu) on the rat thorax. Electrophysiological and breathing data were acquired using a 32-channel data acquisition system (TBSI headstage connected to an A-M Systems Model 4000 amplifier with DataWave Sciworks package or an Intan Tech. RHD-2000 system) with a sampling frequency of 30,000 Hz. For spike detection, data were band-pass filtered between 300 and 5,000 Hz.

Odor Delivery—For odorant delivery, a custom-built air-dilution olfactometer was used (Shusterman et al., 2011). Odorants (Sigma-Aldrich) were kept in liquid phase (diluted 1:10 or 1:100 in mineral oil) in dark vials and mixed into the nitrogen stream that was further diluted 1:10 into a constant air stream in the olfactometer. The following odorants were used: amyl acetate, hexanal, orange oil, benzaldehyde, cineol, anisaldehyde, eugenol, and citral. Odorants were delivered in a randomized order with a maximum of three consecutive presentations of the same odorant. Odorants were applied for 500 ms with an intertrial interval of 10 s.

Analysis—Analysis of recorded data was performed using custom-written scripts in Matlab (MathWorks). Only single units with a clear refractory period of the interspike interval were considered. The observed lag between two different respiration measurement methods was subtracted from the infrared signal to align odor responses to the first inhalation after odor onset (Figure S6). M/TC units were initially analyzed by using the Z score of the firing rate (Wolff et al., 2014). The Z score of the firing rate was computed by summing all bins of the peristimulus time histogram (PSTH) for all cells, subtracting the average baseline count, and then dividing the result by the SD of the baseline. Units were considered odor responsive if the response following odor presentation exceeded a Z score of 1.96. Baseline firing rates were determined over 5 s before each odor presentation. Peak odor responses correspond to the highest 100 ms firing rate bin of the PSTH of each cell within 1 s following odor onset. For each unit, three time windows were analyzed for each odor before, during, and following application of TGOT. To examine a change in the signal-to-noise ratio in M/TC firing, we calculated a modulation index for each unit and each condition, defined as $(\text{firing rate}_{\text{response}} - \text{firing rate}_{\text{baseline}})/(\text{firing rate}_{\text{response}} + \text{firing rate}_{\text{baseline}})$. The modulation index ranges from −1 (high baseline activity, low evoked response) to +1 (low baseline, high evoked response). To compute the population PSTHs, the average odor response across all presented odorants was calculated for each unit. Putative GC units were analyzed by using the Z score of the firing rate.

For further Experimental Procedures see Supplemental Information.

Supplementary Material

Refer to Web version on PubMed Central for supplementary material.

Acknowledgments

We thank Patrick Jendritza for help with recordings, Drs. Heike Tost and Georg Köhr for discussions, Dr. Marina Eliava for histology, Cathrin Huber and Christian Gluch for technical assistance, and Dr. Wolfgang Weber-Fahr and Felix Hoerner for structural MRI imaging. The project was funded by DFG KE1661/1-1 and DFG Collaborative Research Center (SFB) 636 to W.K. and the Schaller Research Foundation and DFG SFB 1134 to V.G. W.S.Y. was supported by the intramural research program of the NIMH (ZIA-MH-002498-24).

REFERENCES

Alonso M, Lepousez G, Sebastien W, Bardy C, Gabellec MM, Torquet N, Lledo PM. Activation of adult-born neurons facilitates learning and memory. Nat. Neurosci. 2012; 15:897–904. [PubMed: 22581183]

American Psychiatric Association. Diagnostic and Statistical Manual of Mental Disorders. Fifth. American Psychiatric Association; 2013.

Angelo K, Rancz EA, Pimentel D, Hundahl C, Hannibal J, Fleischmann A, Pichler B, Margrie TW. A biophysical signature of network affiliation and sensory processing in mitral cells. Nature. 2012; 488:375–378. [PubMed: 22820253]

Asperger H. Die autistischen psychopathen im kindesalter. Arch. Psychiatr. Nervenkr. 1944; 177:76–136.

Balu R, Strowbridge BW. Opposing inward and outward conductances regulate rebound discharges in olfactory mitral cells. J. Neurophysiol. 2007; 97:1959–1968. [PubMed: 17151219]

Balu R, Pressler RT, Strowbridge BW. Multiple modes of synaptic excitation of olfactory bulb granule cells. J. Neurosci. 2007; 27:5621–5632. [PubMed: 17522307]

Barlow, HB. Possible principles underlying the transformations of sensory messages. In: Rosenblith, WA., editor. Sensory Communication. M.I.T. Press, Massachusetts Institute of Technology; 1961. p. 217-234.

Beier KT, Steinberg EE, DeLoach KE, Xie S, Miyamichi K, Schwarz L, Gao XJ, Kremer EJ, Malenka RC, Luo L. Circuit architecture of VTA dopamine neurons revealed by systematic input-output mapping. Cell. 2015; 162:622–634. [PubMed: 26232228]

Boyd AM, Sturgill JF, Poo C, Isaacson JS. Cortical feedback control of olfactory bulb circuits. Neuron. 2012; 76:1161–1174. [PubMed: 23259951]

Boyd AM, Kato HK, Komiyama T, Isaacson JS. Broadcasting of cortical activity to the olfactory bulb. Cell Rep. 2015; 10:1032–1039. [PubMed: 25704808]

Brennan PA, Kendrick KM. Mammalian social odours: attraction and individual recognition. Philos. Trans. R. Soc. Lond. B Biol. Sci. 2006; 361:2061–2078. [PubMed: 17118924]

Brunjes PC, Illig KR, Meyer EA. A field guide to the anterior olfactory nucleus (cortex). Brain Res. Brain Res. Rev. 2005; 50:305–335. [PubMed: 16229895]

Cajal, SRy. Histologie du Systéme Nerveux de L'homme et des Vertébrés. 1911; 2 (Maloine).

Cang J, Isaacson JS. In vivo whole-cell recording of odor-evoked synaptic transmission in the rat olfactory bulb. J. Neurosci. 2003; 23:4108–4116. [PubMed: 12764098]

Carey RM, Wachowiak M. Effect of sniffing on the temporal structure of mitral/tufted cell output from the olfactory bulb. J. Neurosci. 2011; 31:10615–10626. [PubMed: 21775605]

Choe HK, Reed MD, Benavidez N, Montgomery D, Soares N, Yim YS, Choi GB. Oxytocin mediates entrainment of sensory stimuli to social cues of opposing valence. Neuron. 2015; 87:152–163. [PubMed: 26139372]

Crane L, Goddard L, Pring L. Sensory processing in adults with autism spectrum disorders. Autism. 2009; 13:215–228. [PubMed: 19369385]

Dantzer R, Bluthe RM, Koob GF, Le Moal M. Modulation of social memory in male rats by neurohypophyseal peptides. Psychopharmacology (Berl.). 1987; 91:363–368. [PubMed: 3104959]

Dantzer R, Tazi A, Bluthé RM. Cerebral lateralization of olfactory-mediated affective processes in rats. Behav. Brain Res. 1990; 40:53–60. [PubMed: 2278657]

Davis BJ, Macrides F, Youngs WM, Schneider SP, Rosene DL. Efferents and centrifugal afferents of the main and accessory olfactory bulbs in the hamster. Brain Res. Bull. 1978; 3:59–72. [PubMed: 75756]

de Olmos J, Hardy H, Heimer L. The afferent connections of the main and the accessory olfactory bulb formations in the rat: an experimental HRP-study. J. Comp. Neurol. 1978; 181:213–244. [PubMed: 690266]

De Saint Jan D, Hirnet D, Westbrook GL, Charpak S. External tufted cells drive the output of olfactory bulb glomeruli. J. Neurosci. 2009; 29:2043–2052. [PubMed: 19228958]

Dölen G, Darvishzadeh A, Huang KW, Malenka RC. Social reward requires coordinated activity of nucleus accumbens oxytocin and serotonin. Nature. 2013; 501:179–184. [PubMed: 24025838]

Domes G, Heinrichs M, Kumbier E, Grossmann A, Hauenstein K, Herpertz SC. Effects of intranasal oxytocin on the neural basis of face processing in autism spectrum disorder. Biol. Psychiatry. 2013; 74:164–171. [PubMed: 23510581]

Doucette W, Gire DH, Whitesell J, Carmean V, Lucero MT, Restrepo D. Associative cortex features in the first olfactory brain relay station. Neuron. 2011; 69:1176–1187. [PubMed: 21435561]

Elands J, Barberis C, Jard S. [3H]-[Thr4,Gly7]OT: a highly selective ligand for central and peripheral OT receptors. Am. J. Physiol. 1988; 254:E31–E38. [PubMed: 2827511]

Engelmann M, Ebner K, Wotjak CT, Landgraf R. Endogenous oxytocin is involved in short-term olfactory memory in female rats. Behav. Brain Res. 1998; 90:89–94. [PubMed: 9520216]

Ferguson JN, Aldag JM, Insel TR, Young LJ. Oxytocin in the medial amygdala is essential for social recognition in the mouse. J. Neurosci. 2001; 21:8278–8285. [PubMed: 11588199]

Fleming A, Vaccarino F, Tambosso L, Chee P. Vomeronasal and olfactory system modulation of maternal behavior in the rat. Science. 1979; 203:372–374. [PubMed: 760196]

Freeman SM, Inoue K, Smith AL, Goodman MM, Young LJ. The neuroanatomical distribution of oxytocin receptor binding and mRNA in the male rhesus macaque (Macaca mulatta). Psychoneuroendocrinology. 2014a; 45:128–141. [PubMed: 24845184]

Freeman SM, Walum H, Inoue K, Smith AL, Goodman MM, Bales KL, Young LJ. Neuroanatomical distribution of oxytocin and vasopressin 1a receptors in the socially monogamous coppery titi monkey (Callicebus cupreus). Neuroscience. 2014b; 273:12–23. [PubMed: 24814726]

Freund-Mercier MJ, Stoeckel ME, Palacios JM, Pazos A, Reichhart JM, Porte A, Richard P. Pharmacological characteristics and anatomical distribution of [3H]oxytocin-binding sites in the Wistar rat brain studied by autoradiography. Neuroscience. 1987; 20:599–614. [PubMed: 3647280]

Haberly LB, Price JL. Association and commissural fiber systems of the olfactory cortex of the rat. II. Systems originating in the olfactory peduncle. J. Comp. Neurol. 1978; 181:781–807. [PubMed: 690285]

Hayar A, Karnup S, Ennis M, Shipley MT. External tufted cells: a major excitatory element that coordinates glomerular activity. J. Neurosci. 2004; 24:6676–6685. [PubMed: 15282270]

Huber D, Veinante P, Stoop R. Vasopressin and oxytocin excite distinct neuronal populations in the central amygdala. science. 2005; 308:245–248. [PubMed: 15821089]

Hurley LM, Devilbiss DM, Waterhouse BD. A matter of focus: monoaminergic modulation of stimulus coding in mammalian sensory networks. Curr. Opin. Neurobiol. 2004; 14:488–495. [PubMed: 15321070]

Igarashi KM, Ieki N, An M, Yamaguchi Y, Nagayama S, Kobayakawa K, Kobayakawa R, Tanifuji M, Sakano H, Chen WR, Mori K. Parallel mitral and tufted cell pathways route distinct odor information to different targets in the olfactory cortex. J. Neurosci. 2012; 32:7970–7985. [PubMed: 22674272]

Insel TR. The challenge of translation in social neuroscience: a review of oxytocin, vasopressin, and affiliative behavior. Neuron. 2010; 65:768–779. [PubMed: 20346754]

Kay LM, Laurent G. Odor- and context-dependent modulation of mitral cell activity in behaving rats. Nat. Neurosci. 1999; 2:1003–1009. [PubMed: 10526340]

Kelsch W, Lin CW, Lois C. Sequential development of synapses in dendritic domains during adult neurogenesis. Proc. Natl. Acad. Sci. USA. 2008; 105:16803–16808. [PubMed: 18922783]

Kendrick KM, Lévy F, Keverne EB. Changes in the sensory processing of olfactory signals induced by birth in sheep. science. 1992; 256:833–836. [PubMed: 1589766]

Kerr DI, Hagbarth KE. An investigation of olfactory centrifugal fiber system. J. Neurophysiol. 1955; 18:362–374. [PubMed: 13243143]

Kim Y, Venkataraju KU, Pradhan K, Mende C, Taranda J, Turaga SC, Arganda-Carreras I, Ng L, Hawrylycz MJ, Rockland KS, et al. Mapping social behavior-induced brain activation at cellular resolution in the mouse. Cell Rep. 2015; 10:292–305. [PubMed: 25558063]

Knobloch HS, Charlet A, Hoffmann LC, Eliava M, Khrulev S, Cetin AH, Osten P, Schwarz MK, Seeburg PH, Stoop R, Grinevich V. Evoked axonal oxytocin release in the central amygdala attenuates fear response. Neuron. 2012; 73:553–566. [PubMed: 22325206]

Kogan JH, Frankland PW, Silva AJ. Long-term memory underlying hippocampus-dependent social recognition in mice. Hippocampus. 2000; 10:47–56. [PubMed: 10706216]

Laaris N, Puche A, Ennis M. Complementary postsynaptic activity patterns elicited in olfactory bulb by stimulation of mitral/tufted and centrifugal fiber inputs to granule cells. J. Neurophysiol. 2007; 97:296–306. [PubMed: 17035366]

Lee HJ, Caldwell HK, Macbeth AH, Tolu SG, Young WS 3rd. A conditional knockout mouse line of the oxytocin receptor. Endocrinology. 2008; 149:3256–3263. [PubMed: 18356275]

Lee HJ, Macbeth AH, Pagani JH, Young WS 3rd. Oxytocin: the great facilitator of life. Prog. Neurobiol. 2009; 88:127–151. [PubMed: 19482229]

Linster C, Fontanini A. Functional neuromodulation of chemo-sensation in vertebrates. Curr. Opin. Neurobiol. 2014; 29:82–87. [PubMed: 24971592]

Lukas M, Neumann ID. Oxytocin and vasopressin in rodent behaviors related to social dysfunctions in autism spectrum disorders. Behav. Brain Res. 2013; 251:85–94. [PubMed: 22981649]

Lukas M, Toth I, Reber SO, Slattery DA, Veenema AH, Neumann ID. The neuropeptide oxytocin facilitates pro-social behavior and prevents social avoidance in rats and mice. Neuropsychopharmacology. 2011; 36:2159–2168. [PubMed: 21677650]

Lukas M, Toth I, Veenema AH, Neumann ID. Oxytocin mediates rodent social memory within the lateral septum and the medial amygdala depending on the relevance of the social stimulus: male juvenile versus female adult conspecifics. Psychoneuroendocrinology. 2013; 38:916–926. [PubMed: 23102690]

Luskin MB, Price JL. The topographic organization of associational fibers of the olfactory system in the rat, including centrifugal fibers to the olfactory bulb. J. Comp. Neurol. 1983; 216:264–291. [PubMed: 6306065]

Madisen L, Zwingman TA, Sunkin SM, Oh SW, Zariwala HA, Gu H, Ng LL, Palmiter RD, Hawrylycz MJ, Jones AR, et al. A robust and high-throughput Cre reporting and characterization system for the whole mouse brain. Nat. Neurosci. 2010; 13:133–140. [PubMed: 20023653]

Markopoulos F, Rokni D, Gire DH, Murthy VN. Functional properties of cortical feedback projections to the olfactory bulb. Neuron. 2012; 76:1175–1188. [PubMed: 23259952]

Markram K, Markram H. The intense world theory—a unifying theory of the neurobiology of autism. Front. Hum. Neurosci. 2010; 4:224. [PubMed: 21191475]

Marlin BJ, Mitre M, D'amour JA, Chao MV, Froemke RC. Oxytocin enables maternal behaviour by balancing cortical inhibition. Nature. 2015; 520:499–504. [PubMed: 25874674]

Meyer-Lindenberg A, Tost H. Neural mechanisms of social risk for psychiatric disorders. Nat. Neurosci. 2012; 15:663–668. [PubMed: 22504349]

Miczek, KA.; de Boer, SF. Aggressive, defensive, and submissive behavior. In: Whishaw, IQ.; Kolb, B., editors. The Behavior of the Laboratory Rat: A Handbook with Tests. Oxford University Press; 2005. p. 344-352.

Mykytowycz R, Goodrich BS. Skin glands as organs of communication in mammals. J. Invest. Dermatol. 1974; 62:124–131. [PubMed: 4206500]

Natynczuk SE, Macdonald DW. Scent, sex, and the self-calibrating rat. J. Chem. Ecol. 1994; 20:1843–1857. [PubMed: 24242712]

Nissant A, Bardy C, Katagiri H, Murray K, Lledo PM. Adult neurogenesis promotes synaptic plasticity in the olfactory bulb. Nat. Neurosci. 2009; 12:728–730. [PubMed: 19412168]

Numan, M.; Insel, TR. The Neurobiology of Parental behavior. Springer; 2003.

Olshausen BA, Field DJ. Sparse coding of sensory inputs. Curr. Opin. Neurobiol. 2004; 14:481–487. [PubMed: 15321069]

Otazu GH, Tai LH, Yang Y, Zador AM. Engaging in an auditory task suppresses responses in auditory cortex. Nat. Neurosci. 2009; 12:646–654. [PubMed: 19363491]

Otazu GH, Chae H, Davis MB, Albeanu DF. Cortical feedback decorrelates olfactory bulb output in awake mice. Neuron. 2015; 86:1461–1477. [PubMed: 26051422]

Owen SF, Tuncdemir SN, Bader PL, Tirko NN, Fishell G, Tsien RW. Oxytocin enhances hippocampal spike transmission by modulating fast-spiking interneurons. Nature. 2013; 500:458–462. [PubMed: 23913275]

Pager J, Giachetti I, Holley A, Le Magnen J. A selective control of olfactory bulb electrical activity in relation to food deprivation and satiety in rats. Physiol. Behav. 1972; 9:573–579. [PubMed: 4670856]

Popik P, Vetulani J, Bisaga A, van Ree JM. Recognition cue in the rat's social memory paradigm. J. Basic Clin. Physiol. Pharmacol. 1991; 2:315–327. [PubMed: 1822146]

Raggenbass M. Vasopressin- and oxytocin-induced activity in the central nervous system: electrophysiological studies using in-vitro systems. Prog. Neurobiol. 2001; 64:307–326. [PubMed: 11240311]

Rinberg D, Koulakov A, Gelperin A. Sparse odor coding in awake behaving mice. J. Neurosci. 2006; 26:8857–8865. [PubMed: 16928875]

Robertson CE, Thomas C, Kravitz DJ, Wallace GL, Baron-Cohen S, Martin A, Baker CI. Global motion perception deficits in autism are reflected as early as primary visual cortex. Brain. 2014; 137:2588–2599. [PubMed: 25060095]

Rothermel M, Wachowiak M. Functional imaging of cortical feedback projections to the olfactory bulb. Front. Neural Circuits. 2014; 8:73. [PubMed: 25071454]

Sanchez-Andrade G, Kendrick KM. The main olfactory system and social learning in mammals. Behav. Brain Res. 2009; 200:323–335. [PubMed: 19150375]

Sánchez-Andrade G, James BM, Kendrick KM. Neural encoding of olfactory recognition memory. J. Reprod. Dev. 2005; 51:547–558. [PubMed: 16284449]

Schoppa NE. AMPA/kainate receptors drive rapid output and precise synchrony in olfactory bulb granule cells. J. Neurosci. 2006; 26:12996–13006. [PubMed: 17167089]

Shipley MT, Adamek GD. The connections of the mouse olfactory bulb: a study using orthograde and retrograde transport of wheat germ agglutinin conjugated to horseradish peroxidase. Brain Res. Bull. 1984; 12:669–688. [PubMed: 6206930]

Shusterman R, Smear MC, Koulakov AA, Rinberg D. Precise olfactory responses tile the sniff cycle. Nat. Neurosci. 2011; 14:1039–1044. [PubMed: 21765422]

Skuse DH, Lori A, Cubells JF, Lee I, Conneely KN, Puura K, Lehtimäki T, Binder EB, Young LJ. Common polymorphism in the oxytocin receptor gene (OXTR) is associated with human social recognition skills. Proc. Natl. Acad. Sci. USA. 2014; 111:1987–1992. [PubMed: 24367110]

Soria-Gómez E, Bellocchio L, Reguero L, Lepousez G, Martin C, Bendahmane M, Ruehle S, Remmers F, Desprez T, Matias I, et al. The endocannabinoid system controls food intake via olfactory processes. Nat. Neurosci. 2014; 17:407–415. [PubMed: 24509429]

Sosulski DL, Bloom ML, Cutforth T, Axel R, Datta SR. Distinct representations of olfactory information in different cortical centres. Nature. 2011; 472:213–216. [PubMed: 21451525]

Stopka P, Janotova K, Heyrovsky D. The advertisement role of major urinary proteins in mice. Physiol. Behav. 2007; 91:667–670. [PubMed: 17477943]

Tribollet E, Barberis C, Jard S, Dubois-Dauphin M, Dreifuss JJ. Localization and pharmacological characterization of high affinity binding sites for vasopressin and oxytocin in the rat brain by light microscopic auto-radiography. Brain Res. 1988; 442:105–118. [PubMed: 2834008]

Vaccari C, Lolait SJ, Ostrowski NL. Comparative distribution of vasopressin V1b and oxytocin receptor messenger ribonucleic acids in brain. Endocrinology. 1998; 139:5015–5033. [PubMed: 9832441]

Viviani D, Charlet A, van den Burg E, Robinet C, Hurni N, Abatis M, Magara F, Stoop R. Oxytocin selectively gates fear responses through distinct outputs from the central amygdala. science. 2011; 333:104–107. [PubMed: 21719680]

Wallenberg A. Anatomie, physiologie und pathologie des sensiblen systems. Dtsch. Z. Nervenheilkd. 1928; 101:111–155.

Wesson DW. Sniffing behavior communicates social hierarchy. Curr. Biol. 2013; 23:575–580. [PubMed: 23477727]

Wiesner BP, Sheard NM. Maternal Behaviour in the Rat (Oliver and Boyd). 1933

Willmore B, Tolhurst DJ. Characterizing the sparseness of neural codes. Network. 2001; 12:255–270. [PubMed: 11563529]

Wolff SB, Gründemann J, Tovote P, Krabbe S, Jacobson GA, Müller C, Herry C, Ehrlich I, Friedrich RW, Letzkus JJ, Lüthi A. Amygdala interneuron subtypes control fear learning through disinhibition. Nature. 2014; 509:453–458. [PubMed: 24814341]

Yamaguchi M, Manabe H, Murata K, Mori K. Reorganization of neuronal circuits of the central olfactory system during postprandial sleep. Front. Neural Circuits. 2013; 7:132. [PubMed: 23966911]

Yoshimura R, Kiyama H, Kimura T, Araki T, Maeno H, Tanizawa O, Tohyama M. Localization of oxytocin receptor messenger ribonucleic acid in the rat brain. Endocrinology. 1993; 133:1239–1246. [PubMed: 8396014]

Yu GZ, Kaba H, Okutani F, Takahashi S, Higuchi T, Seto K. The action of oxytocin originating in the hypothalamic paraventricular nucleus on mitral and granule cells in the rat main olfactory bulb. Neuroscience. 1996; 72:1073–1082. [PubMed: 8735230]

Author Manuscript

Author Manuscript

Author Manuscript

Highlights

- Oxytocin in the olfactory system is required for social recognition
- Oxytocin activates cortical top-down inputs to olfactory bulb interneurons
- Top-down inputs generate states of high signal-to-noise in odor coding

In Brief

Oettl et al. found that oxytocin transforms sensory channels for optimized processing of cues through cortical top-down recruitment of interneurons. These novel oxytocin actions are required for social recognition and may be of relevance to sensory perception deficits in autism.

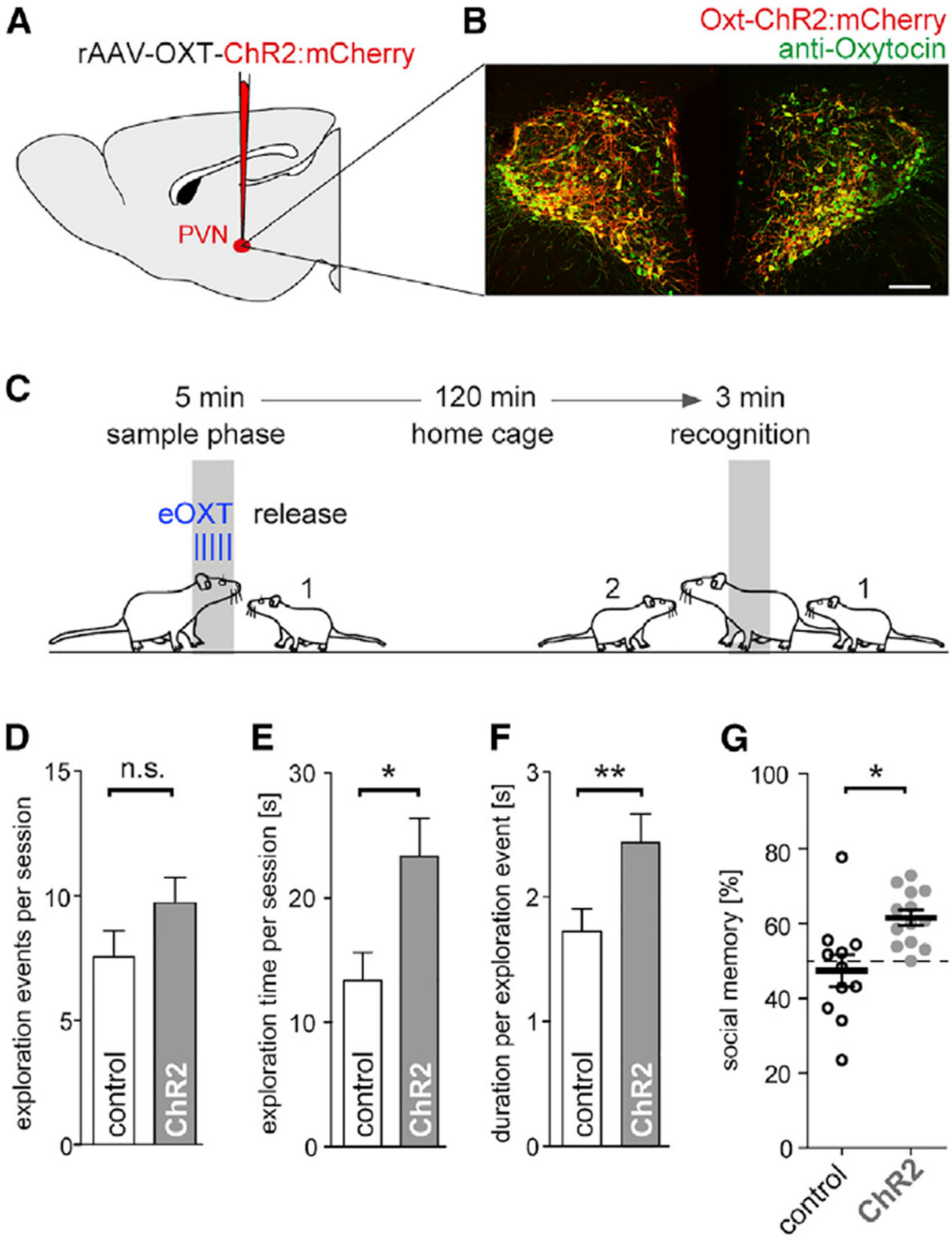

Figure 1. Evoked OXT Release Enhances Exploration and Recognition of Same-Sex Conspecifics

(A) To optogenetically evoke OXT release, we injected an AAV expressing ChR2:mCherry under the control of an OXT promoter fragment, $rAAV_{1/2}$-OXT-ChR2:mCherry, or a control virus, $rAAV_{1/2}$-OXT-GFP, bilaterally into the PVN.

(B) Expression of ChR2:mCherry in the PVN and colocalization with OXT immunoreactivity (scale bar, 150 μm; see also Figure S1).

(C) For the social recognition test, adult female rats were exposed for 5 min to a same-sex juvenile rat (sample phase). After return to the home cage, the adult rat was re-exposed to

the previous and, at the same time, to a novel same-sex juvenile for 3 min (recognition phase).

(D–F) Total number of anogenital exploration events (D), total duration of anogenital exploration (E), and average duration of single anogenital exploration events (F) that 13 $ChR2^+$ or 11 control GFP^+ adult rats performed on the juvenile during the 5 min sample phase (*$p < 0.05$, **$p < 0.01$, t test).

(G) Social recognition memory was expressed as the percentage of time the test animal spent exploring the novel social partner over the total time exploring both same-sex interaction partners for 13 $ChR2^+$ or 11 control GFP^+ adult rats during the 3 min recognition phase (*$p < 0.05$, t test).

All data reported as mean ± SEM.

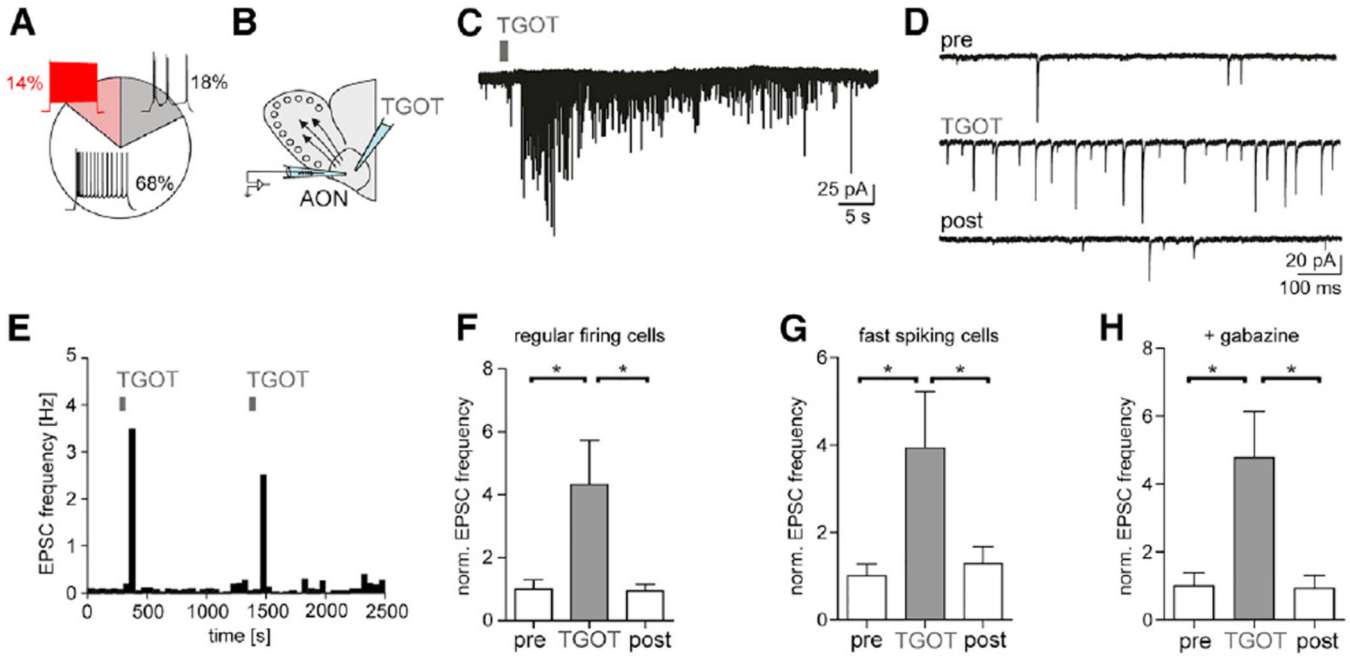

Figure 2. OXTR Activation in the AON Increases the Excitatory Drive

(A) Distribution of 85 neurons with different firing patterns upon intracellular current injection in the AON.

(B) The selective OXTR agonist TGOT (1 μM) was puff applied to the AON.

(C and D) TGOT increased the rate of sEPSCs in a regular-firing neuron at V_h = −60 mV displayed at low (C) and higher temporal resolution (D).

(E) Peristimulus time histogram (PSTH) showed reversible sEPSC rate increases following repeated TGOT application in a regular-firing neuron.

(F) sEPSC rate reversibly increased in 12 AON regular-firing cells following TGOT application. In this and subsequent figures, PSC frequencies were normalized by dividing the PSC rates of the displayed condition by the initial baseline rate (200 s).

(G) TGOT-induced normalized sEPSC rate increases were also observed in six fast-spiking neurons. For burst-firing cells, see Figure S3E.

(H) TGOT still increased normalized sEPSC rate in presence of the $GABA_AR$ antagonist, gabazine (10 μM; n = 4), in regular-firing neurons.

For (F)–(H), $p < 0.05$, ANOVA with posttest indicated *$p < 0.05$.

All data reported as mean ± SEM.

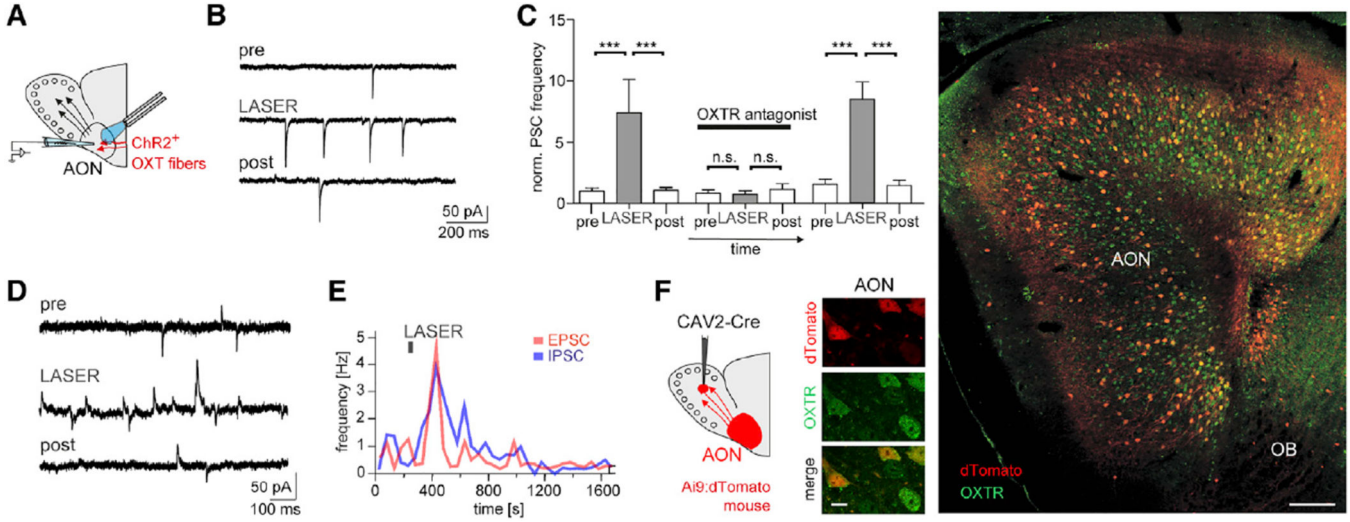

Figure 3. Endogenous OXT Release Also Increases the Excitatory Drive in the AON

(A) In rats expressing ChR2:mCherry in OXT terminals, OXT release was evoked by a burst of blue laser light (30 Hz for 2–20 s).

(B) Laser stimulation resulted in increases of the sEPSC rate in a regular-firing neuron at V_h = −60 mV.

(C) The increase in normalized sPSC rate following repeated laser stimulation was reversibly blocked by the OXTR antagonist OTA (1 μM, n = 6) ($p < 0.05$, ANOVA with posttest indicated ***$p < 0.001$).

(D and E) Simultaneous increases in inward sEPSC and outward sIPSC rate following laser stimulation at V_h = —60 mV(D), and PSTH of the time course of the simultaneous rate increases for a single stimulation in a regular-firing neuron (E).

(F) Retrograde viral labeling of AON neurons following injection of CAV2-Cre into the MOB of Ai9 reporter mice for dTomato, and immunoreactivity for the OXTR (green) in the AON at low and high magnification (scale bar, 10 and 150 μm, respectively).

All data reported as mean ± SEM.

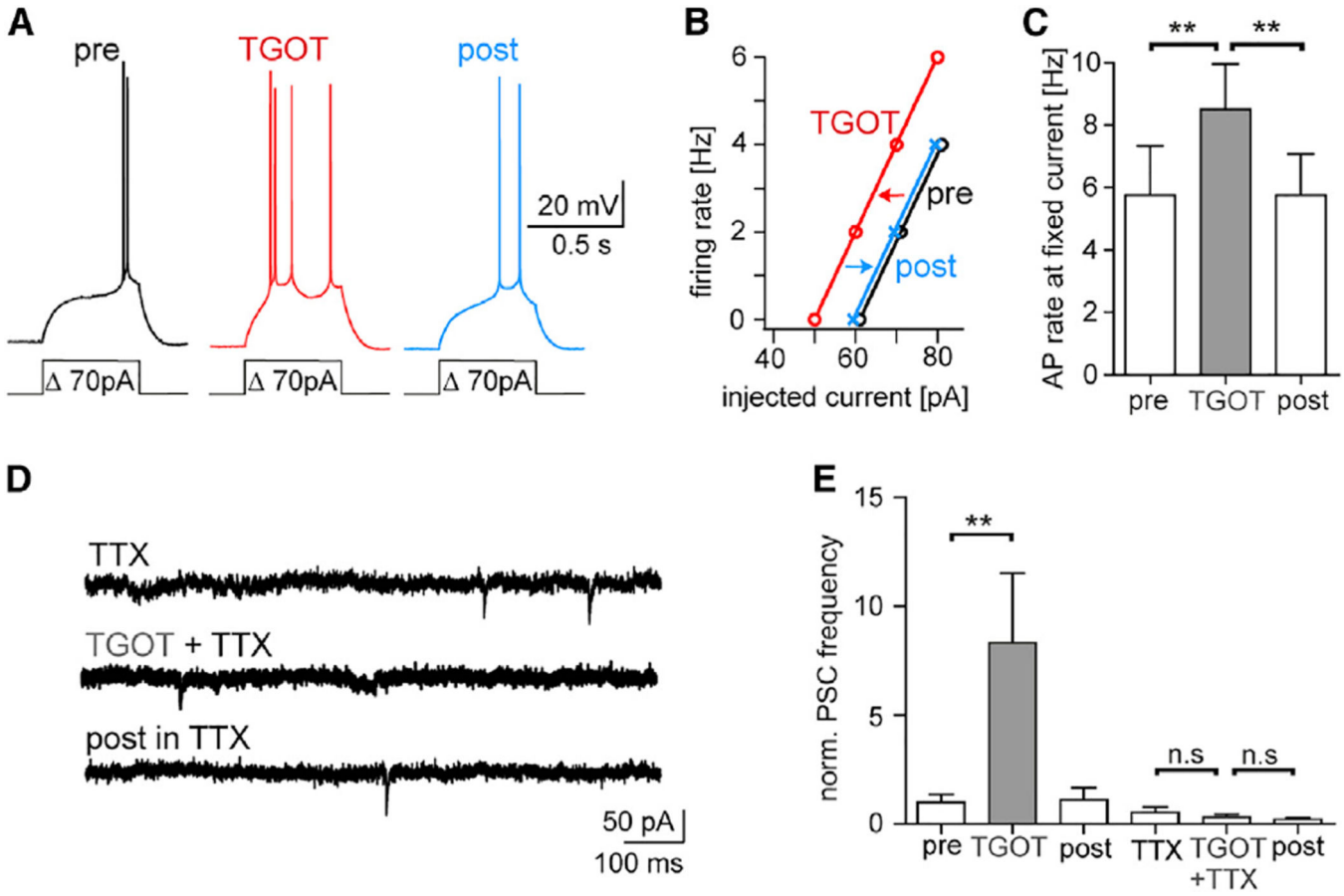

Figure 4. OXTR Activation Increases the Intrinsic Excitability of AON Regular-Firing Neurons

(A) Spike rate transiently increased following application of the OXTR agonist ("TGOT") in presence of CNQX (10 μM), D-AP5 (50 μM), and gabazine (10 μM). The resting membrane potential did not change through TGOT (see Figure S4).

(B) The input-output function for current injection versus spike rate of the cell shown in (A) displayed a reversible parallel shift to the left.

(C) Comparison of the respective spike rate to the same current injection directly after (TGOT) or 5 min after TGOT application (post) (n = 8).

(D) The fast sodium channel blocker TTX (1 μM) blocked the TGOT-induced sEPSC rate increase in a regular-firing neuron at V_h = −60 mV.

(E) In seven regular-firing neurons, TGOT evoked an increase of normalized PSCs that disappeared in presence of TTX.

For (C) and (E), $p < 0.05$, ANOVA with posttest indicated **$p < 0.01$.

All data reported as mean ± SEM.

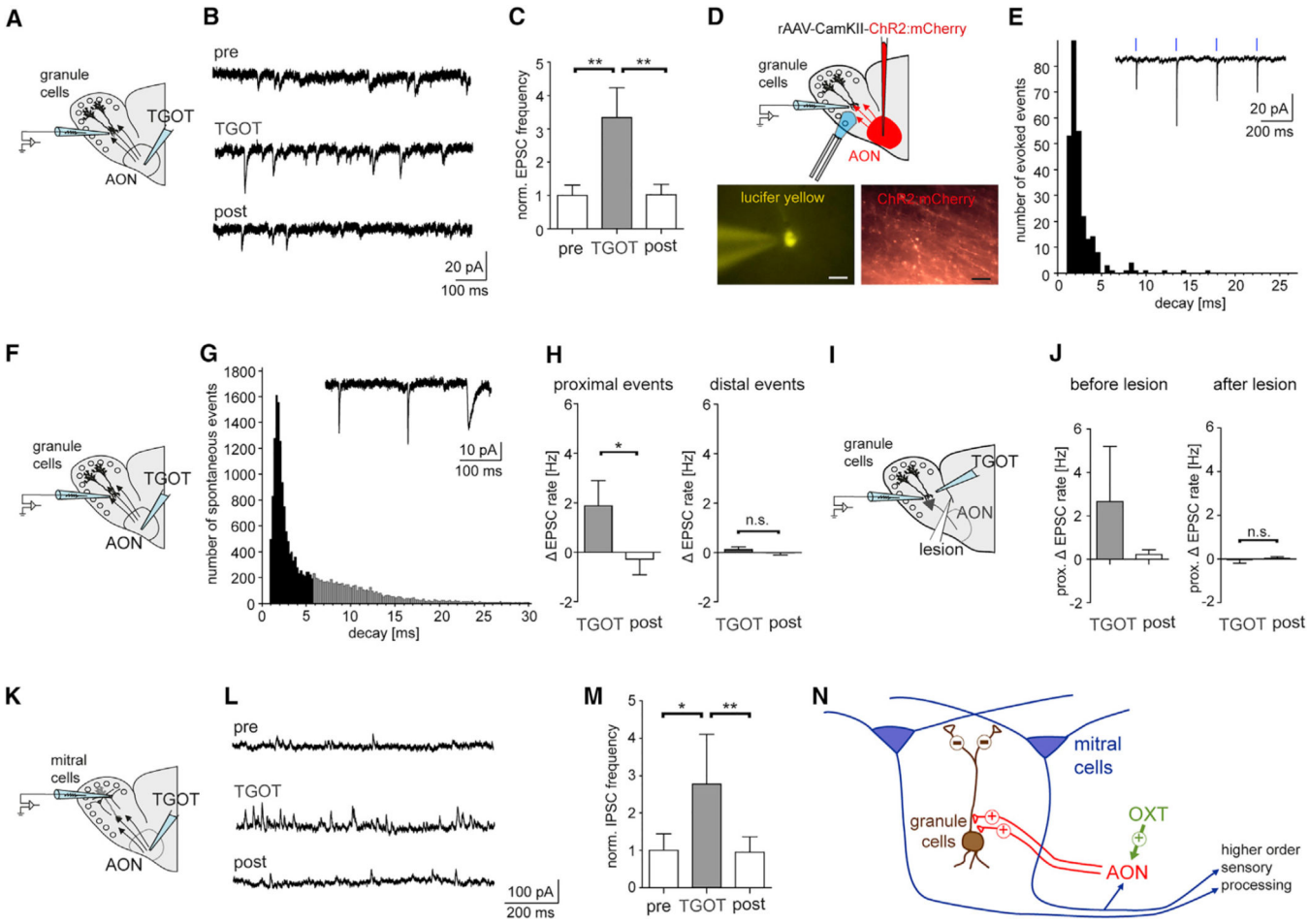

Figure 5. OXTR Activation in the AON Increases Excitatory Drive to GCs and Inhibitory Drive to Mitral Cells in the MOB

(A) The selective OXTR agonist TGOT (1 μM) was puff applied to the AON during recordings from GCs in the MOB.

(B) Recording of sEPSCs (Vh = −60 mV) in a GC.

(C) TGOT reversibly increased the sEPSC rate in seven GCs ($p < 0.05$, ANOVA with posttest indicated $^{**}p < 0.01$).

(D) Glutamatergic top-down projections from the AON to the MOB expressed ChR2:mCherry following injection of $rAAV_{1/2}$-CamKII-ChR2:mCherry in the AON. GCs were filled with Lucifer yellow during recordings (scale bar, 10 μm).

(E) Laser stimulation elicited time-locked EPSCs with fast decay time constants in three GCs at $V_h = -60$ mV.

(F) TGOT was applied to the AON during GC recordings.

(G) sEPSCs were plotted in the histogram, with fast sEPSCs (decay < 6 ms) indicated as black bars.

(H) Analysis of sEPSC decay time constants revealed a selective rate increase of fast (proximal), but not slow (distal), sEPSCs (n = 7 GCs, $^{*}p < 0.05$, t test).

(I) TGOT actions were probed before and after lesioning the projections between the AON and MOB.

(J) TGOT elicited a rate increase of fast sEPSCs. After cutting connection between the AON and MOB, the TGOT response for EPSC rate changes was lost while the baseline rate of sEPSCs was unchanged (n = 5 GCs).
(K) TGOT was applied to the AON during recordings from mitral cells.
(L) Recording of sIPSCs (V_h = −60 mV) in a mitral cell.
(M) TGOT application to the AON elicited a reversible normalized sIPSC rate increase in seven mitral cells at V_h = −60 mV ($p < 0.05$, ANOVA with posttest indicated *$p < 0.05$, **$p < 0.01$).
(N) Scheme summarizing OXT actions in the AON and MOB.
All data reported as mean ± SEM.

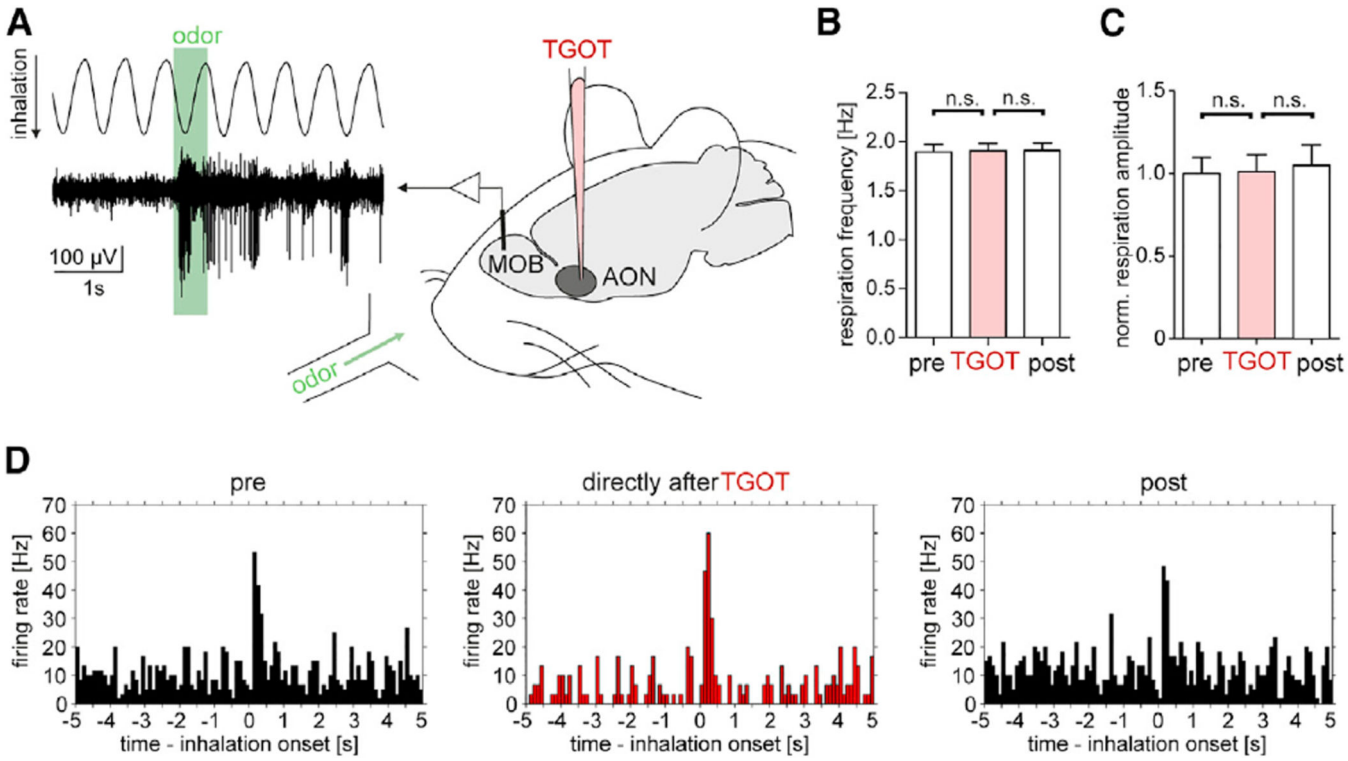

Figure 6. OXTR Activation in the AON Modifies M/TC Firing in the MOB

(A) Experimental setup and example of an extracellular single-unit recording in the MOB of an anesthetized rat. Odorants were applied for 0.5 s and respiration was monitored simultaneously. TGOT (1.6 µM, 1 µL) was applied through a glass micropipette to the AON.

(B and C) Respiration frequency (B) and normalized amplitude (C) did not change with TGOT application in AON (n = 10 recordings) (n.s., ANOVA).

(D) PSTH of M/TC unit firing in response to the same odorant (0.5 s) and effect of TGOT application to AON. Data aligned to sniff onset (bin size, 100 ms) (cf. Figure S6G).

All data reported as mean ± SEM.

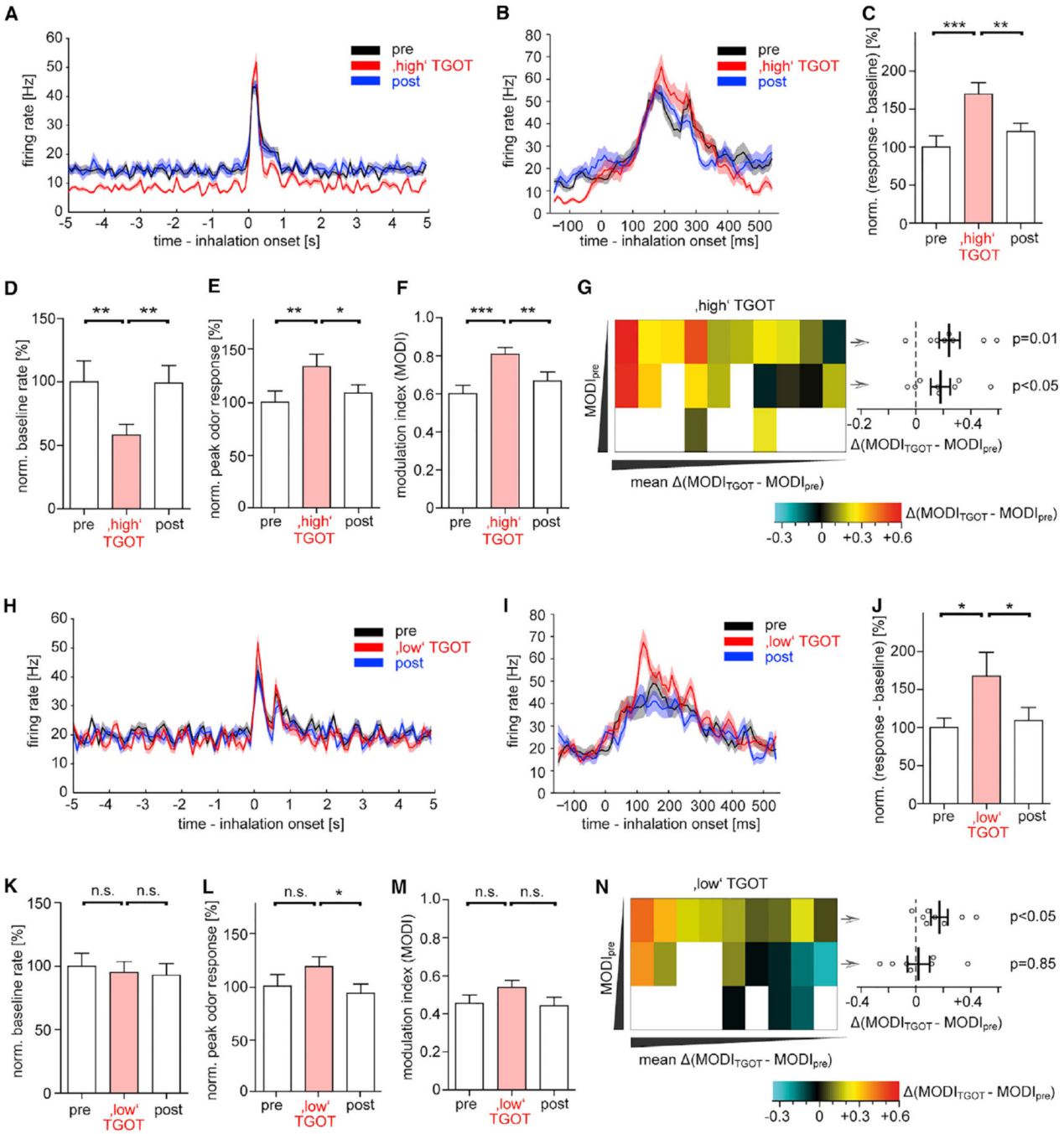

Figure 7. OXTR Activation in the AON Increases Signal-to-Noise Ratios of Odor Responses in M/TCs

(A and B) Average firing rate modulation by the "high" TGOT dose (1 μL of 1.6 μM) in ten M/TCs. Odor-evoked responses increased after TGOT application in AON, whereas baseline firing was reduced. Data were aligned to first inhalation after odor onset with bin sizes of 100 ms (A) or 10 ms (B).

(C) The normalized difference between peak odor response and baseline rate increased upon high TGOT application in 20 cell-odor pairs ($p < 0.05$, ANOVA).

(D) The normalized baseline firing rates of M/TCs decreased following high TGOT in 20 cell-odor pairs ($p < 0.05$, ANOVA).
(E) Normalized peak odor-evoked responses were determined as maximum firing rates of the respective cells within a 100 ms bin within 1 s after odor onset and its increase through high TGOT in 20 cell-odor pairs ($p < 0.05$, ANOVA).
(F) The modulation index (MODI) increased through high TGOT in the 20 cell-odor pairs ($p < 0.05$, ANOVA).
(G) Heat map of the $\Delta(MODI_{TGOT} - MODI_{pre})$ for the 20 cell-odor pairs from the high TGOT sample. Three different odorants had been applied throughout the experiment to each cell. Odors that did not elicit a response in that cell were marked in white. For each cell, odors were ranked according to their increasing $MODI_{pre}$ from top to bottom. Then cells were ranked according to their mean $\Delta(MODI_{TGOT} - MODI_{pre})$ from left to right. Right graph: in the eight cells that responded to more than one odor, $\Delta(MODI_{TGOT} - MODI_{pre})$ increased both for odors with the lowest and next higher $MODI_{pre}$ of each cell (one sample t test), and the increase was similar between the two groups ($p = 0.3$, t test). With all ten cells included for the respective lowest $MODI_{pre}$ $\Delta(MODI_{TGOT} - MODI_{pre}) = 0.24 \pm 0.06$ ($p<0.001$, one sample t test).
(H and I) Average firing rate modulation by the low TGOT dose (1 μL of 0.5 μM) in nine M/TCs. Data were aligned to first inhalation after odor onset with bin sizes of 100 ms (H) or 10 ms (I).
(J) The normalized difference between peak odor response and baseline rate increased upon low TGOT application in 19 cell-odor pairs ($p < 0.05$, ANOVA).
(K) The normalized baseline firing rates of M/TCs did not decrease following low TGOT in 19 cell-odor pairs (n.s., ANOVA).
(L) Normalized peak odor-evoked responses increased through low TGOT in 19 cell-odor pairs ($p < 0.05$, ANOVA).
(M) The change in the modulation index (MODI) through low TGOT did not reach significance for all 19 cell-odor pairs pooled ($p = 0.09$, ANOVA).
(N) Heat map of $\Delta(MODI_{TGOT} - MODI_{pre})$ for the 19 cell-odor pairs from the low TGOT sample. Right graph: in the seven cells that responded to more than one odor, $\Delta(MODI_{TGOT} - MODI_{pre})$ increased only for odors with the lowest $MODI_{pre}$ (one sample t test), and the increase was larger for the lowest than the next higher $MODI_{pre}$ ($p < 0.05$, t test). With all nine cells included for the respective lowest $MODI_{pre}$, $\Delta(MODI_{TGOT} - MODI_{pre}) = 0.19 \pm 0.04$ ($p = 0.002$, one sample t test).
In (C)–(F) and (K)–(N), posttest was indicated *p<0.05, **p<0.01, ***p<0.001.
All data reported as mean ± SEM.

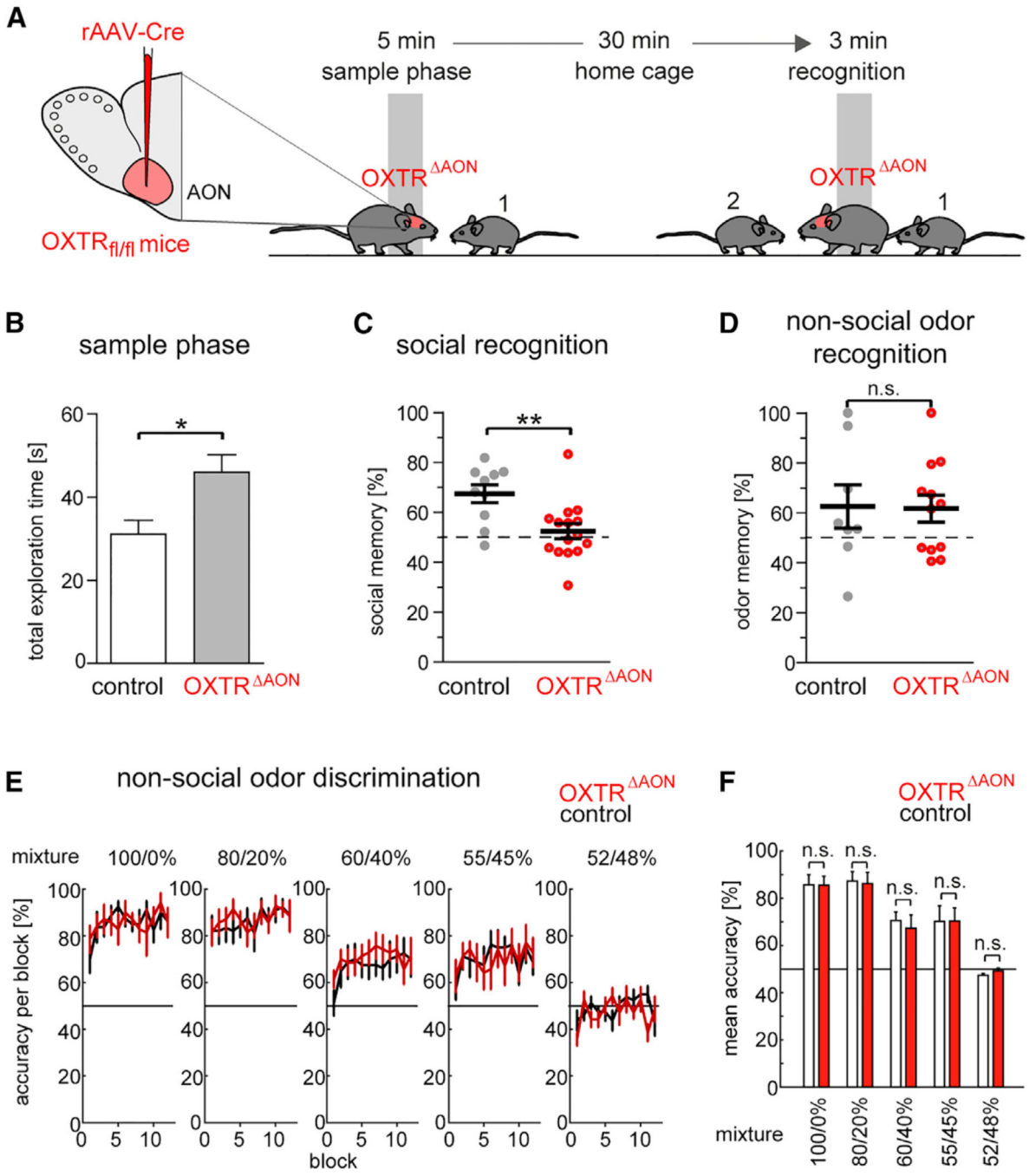

Figure 8. Impaired Same-Sex Social Recognition in Mice Following OXTR Deletion in the AON

(A) Scheme of social recognition test. Male mice were placed with an unknown juvenile for 5 min. After a 30 min interval in the home cage, they were placed with the same juvenile and a second unknown juvenile for 3 min. To generate $OXTR^{\Delta AON}$ mice, $rAAV_{1/2}$-CBA-Cre was injected in the AON of mice in which the OXTR gene was flanked by loxP sites. Control mice received the same virus injection but had two wild-type OXTR alleles.

(B) Total exploration time of social partners during the initial sample phase was longer in 15 $OXTR^{\Delta AON}$ than in 10 control mice (*$p < 0.05$, t test).

(C) Social recognition memory was expressed as the percentage of exploration time of the new juvenile mouse over the total time exploring both interaction partners for 15 $OXTR^{\Delta AON}$ and 10 control mice (**$p < 0.01$, t test).

(D) In an analogous test for nonsocial odors, recognition memory was determined as the percent of exploration time of a new odorant over the total time exploring both odorants for 13 $OXTR^{\Delta AON}$ and 8 control mice (n.s., t test).

(E) Animals were first exposed to pure odorants (“100%”) and then between pairs of increasingly similar mixtures (for instance, 80% (+)-carvone/ 20% (−)-carvone versus 20% (+)-carvone/80% (−)-carvone). Mean percentage of correct responses in each block of 10 trials (120 trials per session) for the carvone enantiomers in 7 control and 8 $OXTR^{\Delta AON}$ mice. A score of 50% corresponds to expected performance at chance level.

(F) Genotype differences determined from the average performance in each session of the odor discrimination (excluding the first 20 trials) for the 7 control and 8 $OXTR^{\Delta AON}$ mice (all t tests $p > 0.44$). All data reported as mean ± SEM.